NMR line shapes in highly polarized large ^{6}LiD target at 2.5 T

J. Koivuniemi[a,*], J. Ball[b], G. Baum[c], P. Berglund[a], N. Doshita[d], F. Gautheron[c], St. Goertz[e], N. Horikawa[f], Y. Kisselev[c,e], K. Kondo[d], W. Meyer[e], G. Reicherz[e]

[a] Low Temperature Laboratory, Helsinki University of Technology, 02015 HUT, Finland and Helsinki Institute of Physics, University of Helsinki, Helsinki 00014, Finland
[b] CEA Saclay, DAPNIA, 91191 Gif-sur-Yvette, France
[c] Physics Department, University of Bielefeld, Bielefeld 33501, Germany
[d] Department of Physics, School of Science, Nagoya University, Nagoya 464-8602, Japan
[e] Physics Department, University of Bochum, Bochum 44780, Germany
[f] College of Engineering Chubu University, Kasugai 487-8501, Japan

Abstract

Due to the vanishing quadrupole interaction only a single narrow 2.8 kHz full-width half-maximum nuclear magnetic resonance (NMR) line is observed in the ^{6}LiD target material for deuterium and ^{6}Li with spin 1. The second and fourth moments are obtained from a Memory function fit to the measured NMR signal. The values are compared to the calculations from dipole interaction between nuclei. The NMR line shape during polarization up to +55% and −52% is discussed.
© 2004 Elsevier B.V. All rights reserved.

1. Introduction

The ^{6}LiD target material has a face-centered-cubic crystal structure [1,2]. Due to the cubic symmetry of the local electric field seen by the nuclei the quadrupole interaction vanishes. Thus only one NMR line is observed for D and ^{6}Li with spin 1 and ^{7}Li with spin $\frac{3}{2}$. It has about 2.8 kHz full-width half-maximum at 2.506 T magnetic field at the deuteron resonance frequency of 16 379 kHz. The line shape is determined by the dipole interaction between the neighboring spins [3]. It is simpler than in the case of deuterated butanol used in the SMC experiment [4], where the quadrupole broadening produced double peaked 300 kHz wide lines.

The NMR system and the area method used to determine the nuclear spin polarization is described in detail in Ref. [5]. The total amount of material inside each NMR coil (see Fig. 1) is about 8 mol. From this 0.2% are protons, 42.4% deuterons, 1.4% ^{3}He, 13.3% ^{4}He, 40.8% ^{6}Li and 1.8% ^{7}Li [6]. The NMR line shape is fitted to the Memory function introduced by Lado et al. [7,8]. The fit allows to determine the second and fourth

*Corresponding author. CERN CH 1211, Geneva 23, Switzerland.
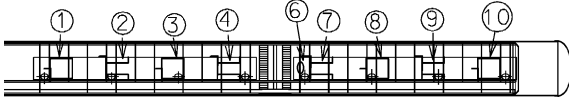E-mail address: jaakko.koivuniemi@cern.ch (J. Koivuniemi).

Fig. 1. Four outer 6 cm long and 3 cm diameter saddle NMR coils are used to measure the polarization of each target cell. These are the 1–4 for upstream and the 7–10 for downstream. Inside the downstream cell the coil 6 is embedded into the target material. Both cells are 60 cm long and have 3 cm diameter.

moments of the average dipole interaction inside the about 1500 granulated beads measured by the coil. The second moment calculated from the dipole interaction is compared with the fitting results for D, ^{6}Li, ^{7}Li and proton.

The Hamiltonian for the spin system contains Zeeman, dipole, quadrupole and hyperfine terms

$$H = H_z + H_{dip} + H_{quad} + H_{hf}. \tag{1}$$

In the high field limit $\langle H_z \rangle / h \approx 16$ MHz is much larger than the internal interaction terms. At the maximum polarization of about 57% obtained for deuterium in the ^{6}LiD at 2.5 T the spin temperatures are around 0.5–1 mK. The thermal energy of the spin system is then $\sim h(10\text{–}20)$ MHz, which is much larger than the internal interaction terms H_{dip}, H_{quad} and H_{hf}, but comparable to the Zeeman term. Thus the thermodynamics of the system is dominated by the Zeeman reservoir, while the interaction terms determine the line shape. In the following, the hyperfine interaction between the nuclei and the free electrons is neglected. Due to the small amount of point defects in the lattice, about 10^{-4}–10^{-3} per nucleus [2,9], the quadrupole term can also be neglected.

In absence of conduction electrons the dipole interaction has the simple form [10]

$$D_{zz,jk} = \frac{\mu_0 \hbar \gamma_j \gamma_k}{4\pi r_{j,k}^3} (1 - 3\cos^2\theta_{j,k}) \tag{2}$$

where $r_{j,k}$ is the distance between the two nuclei and $\theta_{j,k}$ the angle between the external magnetic field and the position vector between the nuclei. γ_j and γ_k are the gyromagnetic ratios of the two nuclei. The distance between neighboring spins is half of the lattice constant or 0.2 nm. Eq. (2) corresponds to a frequency shift of ~ 0–± 1000 Hz.

2. Second and fourth moments

The second moment is the sum of the squared frequency shifts from the dipole interaction with neighboring nuclei

$$M_2^j = g_I \sum_k D_{zz,jk}^2 + g_S \sum_l D_{zz,jl}^2. \tag{3}$$

Here g_I is $3I(I+1)/4$ for like spins and g_S is $S(S+1)/3$ for unlike spins [10]. I is the spin number of the nucleon in consideration and S the spin number of the neighboring unlike nuclei.

The second moments are estimated from Eq. (3) for deuterium, ^{6}Li, ^{7}Li and proton. Calculation was done for a nucleon in center of $11 \times 11 \times 11$ cube of neighboring nuclei. The isotopic dilution 4.2% of ^{7}Li in ^{6}Li and 0.5% proton in deuterium [5] was taken into account by randomly replacing the nucleon with different isotope using the appropriate probability. The target material beads inside the coils have a random crystal direction with respect to external magnetic field. The moments from the randomly chosen 1500 crystal directions were averaged. The results are shown in Table 1.

Calculation of fourth or even higher moments, see for example Refs. [8,10], is much more difficult than the second moment. The fourth moment gives essential information about the line shape and the second moment alone is seldom sufficient [10]. We get the fourth moment from the fit to the measured line shape as shown below.

3. Memory function fit

While the Gaussian line shape is a fairly good approximation for simple line shapes, it takes into account only the second moment. A better approximation is the so-called Memory function which is the solution of the free-induction-decay integro-differential equation [7,8]. The line shape expression for the Memory function is

$$M(\omega) = A \frac{K'(\omega)}{(\omega - K''(\omega))^2 + K'(\omega)^2} \tag{4}$$

Table 1
Typical moments from a Memory function fit at high polarization for deuterium, ^{6}Li, ^{7}Li and proton

	pol (%)	$M_{2\mathrm{calc}}$ (kHz^2)	M_2 (kHz^2)	M_4 (kHz^4)	μ
D outside coils	−49.9/+51.2	1.6	2.5	31	5.0
D embedded coil	+50.2		4.0	85	5.3
^{6}Li outside coils	−48.5/+50.6	1.5	2.2	26	5.4
^{6}Li embedded coil	+51.7		3.5	67	5.5
^{7}Li outside coils	−94.0/+96.6	8.4	14	910	4.6
^{7}Li embedded coil	—		21	2200	5.0
p outside coils	—	53	460	1.6×10^6	7.6
p embedded coil	—		410	1.3×10^6	7.6

The magnetic field was tuned to match the resonance frequency of the Q-meter for each isotope. The moments M_2 and M_4 were averaged for the upstream 1–4 and downstream 7–10 coils. The average polarization for upstream and downstream is shown. $M_{2\mathrm{calc}}$ is the second moment estimated from the nuclear dipole interaction and $\mu = M_4/M_2^2$ is the line shape parameter. For the proton only signals with positive polarization are considered. The polarization of protons is not given due to difficulties in thermal equilibrium calibration.

$$K'(\omega) = \frac{M_2\sqrt{\pi}}{\sqrt{2N_2}} \exp\left(-\frac{\omega^2}{2N_2}\right) \qquad (5)$$

$$K''(\omega) = \frac{M_2\omega}{N_2} \exp\left(-\frac{\omega^2}{2N_2}\right) F\left(\frac{1}{2}, \frac{3}{2}, \frac{\omega^2}{2N_2}\right) \qquad (6)$$

with $N_2 = M_2(\mu - 1)$, $\omega = 2\pi(f - f_0)$ and $\mu = M_4/M_2^2$. Here f_0 is the center frequency of the NMR line and $F(\cdots)$ is a confluent hypergeometrical function. In the case of a simple Gaussian fit the line shape parameter μ is 3. For higher values the line shape becomes more Lorentzian.

4. Measured NMR signals

The continuous wave NMR measurement was done with series-tuned Liverpool Q-meters at fixed magnetic field by sweeping the frequency ± 50 kHz around the nuclear magnetic resonance at 16 379 kHz [5]. The coils are shown in Fig. 1. For Gaussian line shape the line width can be estimated to be $\Delta f = \sqrt{8\ln 2 M_2}$. From the line widths seen in Fig. 2 second moment of about 1.2–1.4 kHz^2 can be expected for deuterium and ^{6}Li while for ^{7}Li it would be about 7.6 kHz^2. With the Memory function fit as seen in Fig. 3 these values become somewhat larger. The values for the different nuclei are summarized in Table 1. There
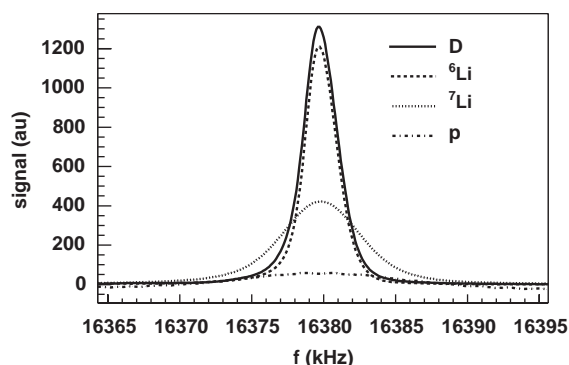
Fig. 2. The measured NMR signals of deuterium at 2.506 T, ^{6}Li at 2.614 T and ^{7}Li at 0.9899 T. The signal from protons at 0.3873 T is very small. It was scaled by factor 5 to make it more visible. The deuterium and ^{6}Li polarizations were about −50%, while ^{7}Li has already −95% polarization. The full-width half-maximum for deuterium is 2.8, 2.6 kHz for ^{6}Li and 6.5 kHz for ^{7}Li.

is a clear difference between the outside coils and the embedded coil. The second moment of the embedded coil is about 1.5 larger than for the outside coils for all nuclei except for protons.

5. Line shapes during polarization

The deuterium NMR line shapes for different polarizations are plotted in Fig. 4. The signals
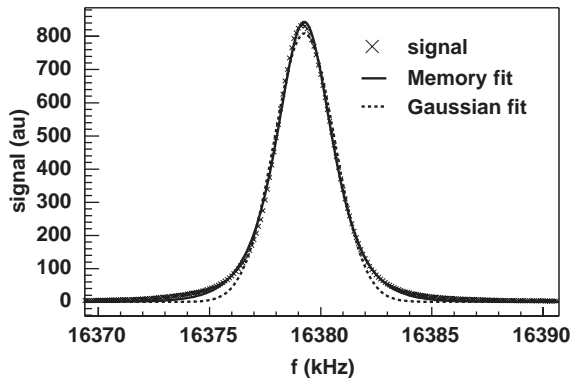
Fig. 3. Deuterium NMR signal measured with outside coil 9 (-40.8% polarization) with a fit to the Memory function (solid line). For comparison also a fit to a simple Gaussian is shown (dashed line). The fit gives a second moment of 2.7 kHz^2 and a 4th moment of 35 kHz^4. From the fitted area polarization of -38.9% can be calculated while the area of Gaussian fit gives -37.0%. The Gaussian fit gives an underestimated second moment of 1.8 kHz^2.
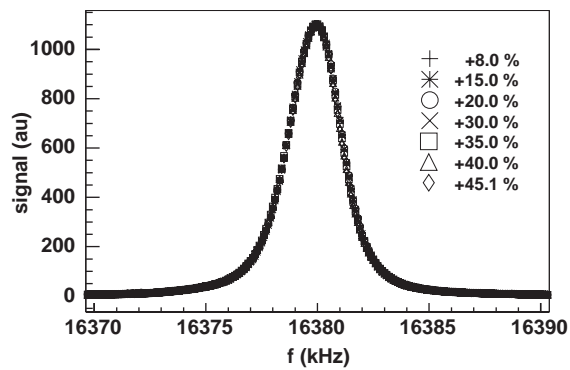

Fig. 4. Comparison of the deuterium signals with polarizations from $+8.0\%$ to $+45.1\%$ measured by the external coil 1. The integrated surface areas agree within 2% with each other. The data were taken in a period of 3 days. The second and fourth moments are between 2.4 and 2.6 kHz^2 and 28 and 34 kHz^4.

have been shifted to the same center frequency and were scaled to have the same surface areas. The line width does not seem to depend on the polarization. The second moment and line-shape parameter μ for deuterium during a typical dynamic nuclear polarization process are shown in Fig. 5. The behavior is not reproducible and looks different for each build-up or relaxation measurement. The fluctuation can be attributed to the spatial non-equilibrium spin temperature in the
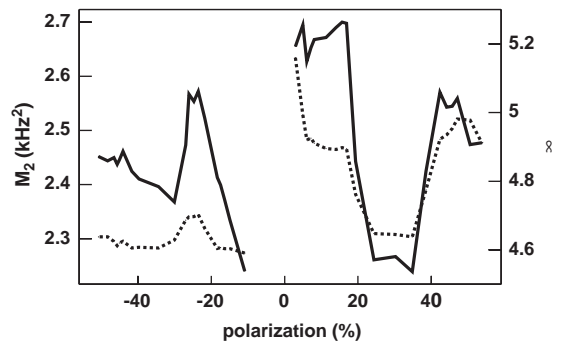

Fig. 5. Second moment M_2 (solid line) and line-shape parameter $\mu = M_4/M_2^2$ (dashed line) during typical polarization build-up. The M_2's and μ's for the upstream coils 1–4 with negative polarization and the downstream coils 7–10 with positive polarization were averaged. The second moments of all individual coils stay between 2.0 and 3.0 kHz^2 during the polarization.
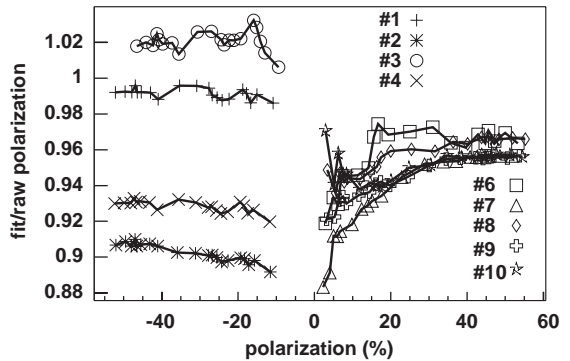

Fig. 6. Ratio of the polarization calculated from the fitted signal and the polarization calculated from the raw signal for the upstream coils 1–4 and the downstream coils 6–10. The average ratio for upstream is the same as the 0.96 of downstream.

system during the polarization or to possible instabilities in the Q-meter.

The polarization from the raw NMR signals is compared to the polarization calculated from the area of the fitted Memory function in Fig. 6. For all downstream coils 6–10 the ratio between these values is very close to 0.96 while for upstream coils 1–4 there is a clear spread. Similar behavior was seen also when the upstream coils were measuring positive polarization and downstream coils negative polarization. The reason for the spread is a

parasitic coupling between the upstream coils [5]. All the coils are measured simultaneously. Corrections (-6–$+5\%$) to the measured polarizations for the upstream coils 1–4 can be done from Fig. 6, but this does not change the average upstream polarization.

6. Discussion

The NMR line shapes of ^{6}LiD can be directly compared with the well developed microscopic theory of dipolar line broadening in solids. It is demonstrated than the line shapes can deviate from the expected ones due to imperfections in the Q-meter measurement. This was seen as larger spread in the systematic error in the upstream coils when comparing the polarization obtained from the raw signals to that integrated from the fitted signal. About 4% of difference in the areas between the fitted and the measured line shapes is observed. The fitting could be improved by taking into account higher moments or by more precise modeling of the coupling of the individual crystals to the NMR coil.

The NMR-lines are wider than expected from the simple model of dipole interaction between the nuclei. The inhomogeneity of the radio frequency field produced by the coils and the local static field are the most probable reasons for this difference. The 1.5 times larger second moment of the embedded coil compared to the outside coil supports this idea. The static field inhomogeneity produced maximum 700 Hz shifts between the center frequencies of the NMR lines measured by the different coils with the same sign of polariza-tion. The coupling between the nuclei and the free electrons is important in the dynamic nuclear polarization and in the spin magnetization relaxation. It could also contribute to the small fluctuations seen in the line shape during the polarization build-up. Third reason for the discrepancy is the continuous wave excitation while the Memory function was derived for free-induction-decay signals.

The line width seen for the small amount of protons is much too large to be explained by the dipole interaction inside the crystal. Thus the measured proton signal comes from hydrogen in the different construction materials used in the target cells or from water adsorbed on the ^{6}LiD crystals.

References

[1] V. Bouffard, Y. Roinel, P. Roubeau, A. Abragam, J. Phys. 41 (1980) 1447.
[2] A. Meier, Ph.D. Thesis, University of Bochum, Germany, 2001.
[3] J.H. Van Vleck, Phys. Rev. 74 (1948) 1168.
[4] C. Dulya, et al., Nucl. Instr. and Meth. A 398 (1997) 109.
[5] K. Kondo, et al., Nucl. Instr. and Meth. A, (2004) these proceedings.
[6] S. Neliba, et al., Nucl. Instr. and Meth. A, (2004) these proceedings.
[7] F. Lado, J.D. Memory, G.W. Parker, Phys. Rev. B 4 (1971) 1406.
[8] M. Mehring, Principles of High Resolution NMR in Solids, 2nd Edition, Springer, Berlin, Heidelberg, 1983.
[9] J. Ball, et al., Nucl. Instr. and Meth. A 498 (2003) 101.
[10] A. Abragam, The Principles of Nuclear Magnetism, Oxford University Press, Hong Kong, 1989.